Chem. Senses 34: 547–557, 2009

doi:10.1093/chemse/bjp031
Advance Access publication June 12, 2009

Enhancement of Odorant-Induced Responses in Olfactory Receptor Neurons by Zinc Nanoparticles

Nilmini Viswaprakash, John C. Dennis, Ludmila Globa, Oleg Pustovyy, Eleanor M. Josephson, Patrick Kanju, Edward E. Morrison and Vitaly J. Vodyanoy

Department of Anatomy, Physiology, and Pharmacology, Auburn University, 109 Greene Hall, Auburn, AL 36849, USA

Correspondence to be sent to: Vitaly Vodyanoy, Department of Anatomy, Physiology, and Pharmacology, Auburn University, 109 Greene Hall, Auburn, AL 36849, USA. e-mail: vodyavi@auburn.edu

Abstract

Zinc metal nanoparticles in picomolar concentrations strongly enhance odorant responses of olfactory sensory neurons. One- to 2-nm metallic particles contain 40–300 zinc metal atoms, which are not in an ionic state. We exposed rat olfactory epithelium to metal nanoparticles and measured odorant responses by electroolfactogram and whole-cell patch clamp. A small amount of zinc nanoparticles added to an odorant or an extracellular/intracellular particle perfusion strongly increases the odorant response in a dose-dependent manner. Zinc nanoparticles alone produce no odor effects. Copper, gold, or silver nanoparticles do not produce effects similar to those of zinc. If zinc nanoparticles are replaced by Zn^{+2} ions in the same concentration range, we observed a reduction of the olfactory receptor neuron odorant response. Based on these observations, we hypothesize that zinc nanoparticles are closely located to the interface between the guanine nucleotide-binding protein and the receptor proteins and are involved in transferring signals in the initial events of olfaction. Our results suggest that zinc metal nanoparticles can be used to enhance and sustain the initial olfactory events.

Key words: cAMP, electroolfactogram, G-protein, metal nanoparticles, metals, whole-cell recording, zinc

Introduction

The initial olfactory transduction events occur in the receptor neuron cilia where receptor proteins bind odorants (Buck and Axel 1991). Odorant binding is followed by activation of heterotrimeric guanine nucleotide–binding proteins (G-proteins) (Anholt et al. 1987; Jones and Reed 1989) and effector enzymes (Pace et al. 1985; Sklar et al. 1986; Bakalyar and Reed 1990). Two effector enzymes, G-protein–coupled adenylyl cyclase (AC) and phospholipase C, were proposed to control primary olfactory neuron responses to odor stimulation in invertebrates and vertebrates (Fadool and Ache 1992; Breer 1994). Excitatory reactions involving 3′-5′-cyclic adenosine monophosphate (cAMP) and inositol triphosphate pathways are well explored, but the receptor protein to G-protein signal transduction mechanism is unknown. Turin (1996) suggested that zinc ion–binding sites are present on both the odorant receptor protein and the G-protein and that zinc ions assist the signal transfer from receptor to G-protein. A general theoretical model (Brookes et al. 2007) examined the plausibility of Turin's proposal and found that it was consistent with the underlying physics and observed features of the early olfactory events. The model required that the authors introduce a hypothetical electron donor/acceptor as a reducing/oxidizing agent in the intracellular fluid, which agent could be zinc ions.

We previously described metallic nanoparticles isolated from human and other vertebrate blood (Samoylov et al. 2005). Those particles contained 40–300 zinc atoms directly bonded with one another in metallic nuclei. In light of our observations and those of Turin (1996) and Brookes et al. (2007), we therefore hypothesized that metallic zinc nanoparticles could be involved in signal transduction between receptor proteins and G-proteins. We demonstrate here that those particles added to a vapor plume enhance the electrical response of olfactory epithelium (OE) in both electroolfactogram (EOG) and single-cell recordings. The effect is dose dependent and reversible (Viswaprakash et al. 2006).

Materials and methods

The primary regulations governing the care and use of animals utilized in this work included the following: the Animal Welfare Act, the National Institute of Health–Public Health

Service policy, and the Guide for the Care and Use of Laboratory Animals.

To establish the specific effects of zinc metal nanoparticles on responses of olfactory sensory neurons to odorants, whole-cell patch-clamp and EOG recordings were made with or without zinc. Rat OEs were dissected and prepared for recording using standard techniques. In the recording chamber, odorants or odorant–metal nanoparticle mixtures were delivered to the OE.

The epithelial slice

An epithelial sample was prepared by the method similar to that described in Sinnarajah et al. (2001). Fragments of septal olfactory mucosa were isolated from rat and placed in the RC-8 Warner Instrument patch-clamp recording chamber so that the basal portions immersed in physiological buffer solution, whereas the apical epithelial surface with olfactory cilia were exposed to the air (Ma et al. 1999).

Odorant mixture

Odorants were purchased from Sigma-Aldrich. An odorant mixture containing 16 mM each ethyl butyrate, eugenol, and (+) and (–) carvone in water was mixed with a vortex and then serially diluted. Concentrations of 1, 2, 4, 8, and 16 mM in water were prepared for EOG and whole-cell recordings. Odorant mixtures at each concentration were kept in 100-mL dark glass bottles, and the odorant mixtures contained in the bottle headspaces were directed to the mixing chamber for mixing with the charcoal-purified air. The prepared mixtures were then applied through a calibrated multibarrel pipette and a small glass nozzle to the surface of the isolated OE.

Metal nanoparticles

Production of protein nucleating centers (PNCs) from shark's blood was described (Samoylov et al. 2005). PNCs are comprised of 1- to 2-nm metallic nanoparticles of various metals, including zinc. The system for metal nanoparticle production from solid metals (Kruyt 1952) consists of a water container and a high-voltage generator with 2 metal electrodes submerged in water. By controlling the voltage and distance between electrodes, the plasma created under water produces a very fine dispersion of metal nanoparticles. Two 2-mm diameter metal electrodes (Alfa Aesar, 99.9999%) were positioned ~6 cm apart in a large Pyrex jar 1 mm below the air–water interface of 850 mL purified (Milli-Q) water that had been autoclaved (23 psi, 120 °C) and chilled to 25 °C. The jar was placed in a running water bath to prevent overheating. A voltage of 15 000 V was applied to the electrodes and was sustained for 12 h. The Zn suspension was collected in a 1-L glass beaker and placed in a refrigerator for 12 h to allow the large metal particles to sediment. The supernatant was transferred to tubes and centrifuged at 40 000 × g for 90 min at 18 °C. After centrifugation, the pellet was discarded. That process was repeated 2 more times, and the final supernatant was subjected to analysis and particle counting. The centrifuge speed and time required to enrich suspensions of nanoparticles smaller than 2 nm were estimated with a Stock's equation (Kruyt 1952).

The colloidal zinc suspensions obtained from Purest Colloids, Inc., and Indigenous Products were used as alternative sources of zinc nanoparticles. Suspensions were filtered through 0.22-μm Fisherbrand Syringe Filters and centrifuged at 40 000 × g for 90 min at 18 °C. Mean zinc nanoparticle concentrations were estimated by UV absorption measured with a DU640 Beckman UV spectrophotometer. Centrifugation rendered a significant narrowing of the UV absorption bandwidth, which indicated an improved uniformity in nanoparticle size. Analysis of nanoparticles was similar to that described in Samoylov et al. (2005). The total concentration of metal in suspension was measured by atomic absorption spectra (GTW Analytical Services). Aliquots of the suspension were dried onto coated grids, and the particles were counted in dark field transmission electron microscope images. Detailed structures were characterized by selected area diffraction as well as nanobeam diffraction (Samoylov et al. 2005). The suspension was kept at 5 °C before use. The nanoparticle concentration is defined as the number of particles per liter of suspension. The number of particles per liter divided by Avogadro number represents the molar particle concentration. Zinc nanoparticle concentrations, determined by particle counting and UV spectra analysis, were used for calculations and labeled "total zinc concentration" later in the text.

Delivery of odorants and metal nanoparticles

For stimulation, a 0.25-s pulse of the odorant mixture at 8 psi was formed by a computer-controlled Pneumatic PicoPump PV800 (World Precision Instruments [WPI]). A pulse of positive pressure drove the odorant into a calibrated multibarrel pipette fitted with a glass nozzle directed at the OE. Each pipette barrel can pass a puff of distinct odorant composition and concentration. The residual odorant was cleared by air between each stimulus application. The odorant pulse patterns were initiated manually at predetermined time intervals or automatically by computer. The automatic computer routine was composed of 0.25-s pulses at 20- and 60-s intervals for EOG and whole-cell experiments, respectively. One series of 10 pulses at 20-s intervals constituted one "EOG recording" and one 15 pulses series at 60-s intervals represented one "whole-cell recording." Thus, in the automatic regime, the single EOG recording had a duration of 200 s and could correspond to 10 response traces. Likewise, the whole-cell computer routine during one whole-cell recording could produce 15 traces over 15 min. These recordings were repeated as many times as needed to cover a desirable number of pulses and duration for a single experiment.

Three methods were used to deliver metal nanoparticles. 1) A nanoparticle suspension was mixed with odorant

solutions to make final nanoparticle concentrations of a few fM to 450 pM. During the puff, the odorant vapor containing metal nanoparticles was delivered to the OE surface. This method is used for both EOG and whole-cell recording. In some EOG experiments, zinc metal nanoparticles were replaced with Zn^{+2} ions at concentrations of 10^{-9}–10^{-15} M, combined with odorants, and delivered to the OE. 2) Metal nanoparticles (5 nM) were added to the EOG recording pipette saline solution. A concentration gradient is formed around the contact point of the pipette tip with the OE. Over time, the nanoparticle concentration increases in the vicinity of contact until recording is terminated or a steady state is attained. 3) Metal nanoparticles (5 nM) were added to the patch-clamp recording pipette saline solution. As above, the nanoparticles diffuse through the pipette opening inside the cell when contact with an olfactory receptor neuron is made. The very tip of the patch pipette was filled with the solution containing no nanoparticles. To estimate the tip fill and diffusion time, the tip was filled with 1% solution of Alcian blue and photographed. The process of the tip filling and the change of the fill level of the pipette (8–16 MΩ) were recorded by a video camera attached to an Olympus BX51 microscope (×40 long working distance objective).

Electroolfactogram

Rat septal OE was placed in a perfusion chamber in physiological buffer (containing 137 mM NaCl, 5.3 mM KCl, 4.2 mM $NaHCO_3$, 0.4 mM KH_2PO_4, 3.4 mM Na_2HPO_4, and 5.6 mM D-glucose at pH 7.4). All EOG recordings were performed in saline lacking divalent cations except for 3 control experiments carried out to test whether or not divalent cations would alter zinc nanoparticle effects. Control experiments were carried out in buffer containing Ca and Mg ions (137 mM NaCl, 5.3 mM KCl, 4.2 mM $NaHCO_3$, 0.4 mM KH_2PO_4, 3.4 mM Na_2HPO_4, 1.3 mM $CaCl_2$, 0.2 mM $MgSO_4$, and 5.6 mM D-glucose at pH 7.4). This buffer was used in both the bathing solution and the recording pipette, and the tissue samples were never exposed to the Ca-free and Mg-free solutions.

The EOG recording electrode, a Ag/AgCl wire in a glass pipette of approximately 24-μm tip opening, was filled with the same physiological buffer and then connected to an electronic amplifier to detect OE responses. Glass pipettes were fabricated using borosilicate capillaries (WPI) and pulled using a P-87 pipette puller (Sutter Instruments). Once contact between the electrode and the OE surface was formed, odorant puffs were applied. Responses over a several-minute time course were amplified by a 700A MultiClamp Amplifier (Axon Instruments), filtered at 2–5 kHz, and recorded.

Whole-cell recording

Current responses were measured with a patch-clamp amplifier (700A MultiClamp Amplifier, Axon Instruments) in the whole-cell configuration (Sinnarajah et al. 2001). Odorant–zinc particle vapor mixture containing equal parts of ethyl butyrate, eugenol, and (+) and (–) carvones was delivered with dried, purified air by a Pneumatic PicoPump PV800 (WPI). In our experience with patch clamp, we obtain better electrode membrane seals and superior stability with Ca- and Mg-free Hank's buffer. Therefore, in the recording chamber, the tissue was perfused with a bathing solution that contained 136.9 mM NaCl, 5.3 mM KCl, 4.2 mM $NaHCO_3$, 0.4 mM KH_2PO_4, 3.4 mM Na_2HPO_4, and 5.6 mM D-glucose at pH 7.4. The patch electrode (resistance of 8–16 MΩ) was filled with a solution containing 110 mM KCl, 4 mM NaCl, 2 mM $NaHCO_3$, 1 mM $MgCl_2$, 0.1 mM $CaCl_2$, and 2 mM 3-(morpholino)propansulfonic acid at pH 7.4 with metal nanoparticles. The whole-cell response over the time course of several minutes was recorded after being amplified by the patch-clamp amplifier and filtered at 2–5 kHz. After compensation, the series resistance was always lower than 20 MΩ.

Stability of olfactory responses

Because of large variability of odorant responses by individual cells (Firestein et al. 1993), stability over an extended period and response reproducibility at a single contact were required. We made considerable efforts to correct mechanical and electrical problems that potentially could affect stability of the system. The recording chamber was contained in a grounded Faraday box on a vibration isolation table (GS-34 Newport). Most of the experiments did not last longer than 30 and 60 min for whole cell and EOG, respectively. Olfactory tissues were examined for responsiveness to odorants and stability with no metal nanoparticles added. Repeatable recordings of consecutive 0.25-s odorant mixture pulses were produced at 20- and 60-s intervals in EOG and whole-cell experiments, respectively. For short-term stability, 10 pulses for EOG and 15 pulses for whole-cell experiments were applied. To examine long-term stability and reproducibility, a few extended time EOG and whole-cell experiments were performed.

Results

Stability and repeatability of olfactory responses

Typical EOG and whole-cell responses to odorant pulses are shown in Figures 1 and 2. Most of the experiments in this work were carried out with few electrode–OE contacts and several recordings. Automatic EOG recordings were approximately 80% successful in obtaining 10 response traces per recording. Approximately 60% whole-cell contacts rendered 15 traces per recording. Response amplitude was reasonably stable during repeated odorant application. The results of EOG and whole-cell stability experiments are shown in Tables 1 and 2.

The mean value of the relative change of 2 consecutive EOG peaks stimulated by the same odorant pulse ($|\Delta V/V|$) was 4.5% (0.045 ± 0.010 [standard error {SE}], 10 recordings,

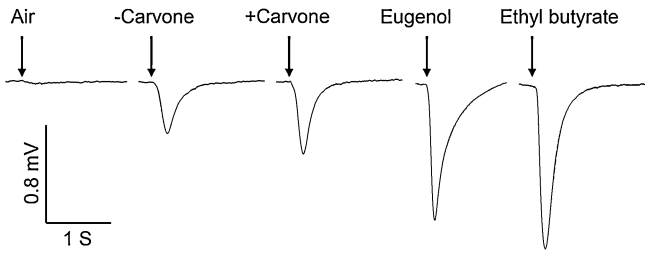

Figure 1 EOG recording from OE responses to individual odorants. The recordings were obtained from the same site on the OE. Pulse interval was 1 min, and 2 pure air–clearing puffs between the odorant pulses were given. The figure shows typical traces obtained with 4 tissues, 7 electrode contacts, and 97 recordings. Each recording comprises 6–10 EOG traces.

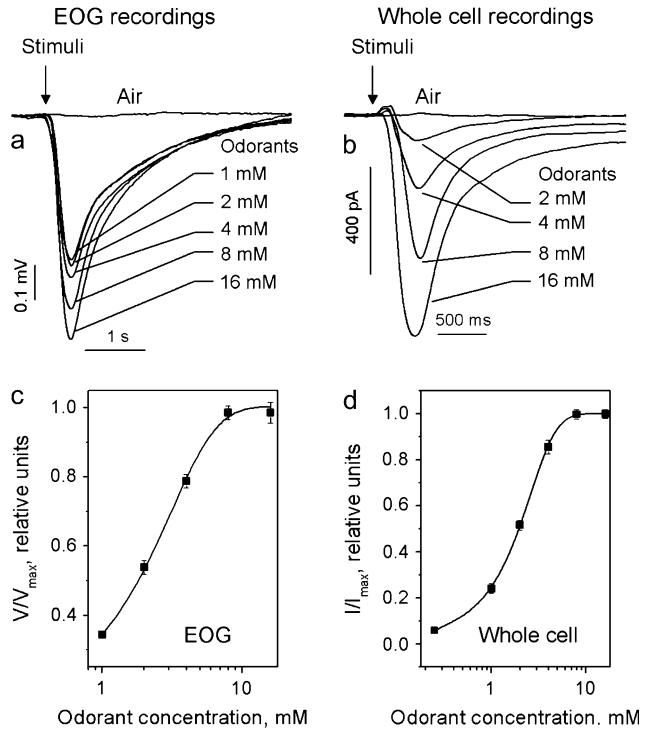

Figure 2 Odorant response recordings from rat OE and a single olfactory neuron. The stimulus was a 0.25-s pulse of air or odorant mixture. **(a)** EOG traces induced by a pure air and odorant mixture at different concentrations. The representative set of traces was obtained from 4 tissues, 10 contacts, and 34 EOG recordings. **(b)** Current traces from whole-cell recordings of olfactory neurons with holding potentials of −70 mV. The stimulus was a 0.25-s pulse of air or odorant mixture. Downward direction indicates inward current. This is a typical representation of 23 whole-cell recordings. Each recording comprises 3–15 whole-cell traces. **(c)** Plot of normalized, peak EOG voltage (V/V_{max}) evoked by odorant versus odorant concentration. **(d)** Plot of normalized, peak negative current (I/I_{max}) evoked by odorant versus odorant concentration.

100 traces). The relative change of whole-cell peak values of 2 consecutive responses stimulated by the same odorant pulse ($|\Delta I/I|$) was 11% (0.11 ± 0.03 [SE], 6 recordings, 90 traces). The drift slopes estimated from 30 min of repeated EOG and whole-cell recording were 0.65 ± 0.10% min^{-1} and 0.75 ± 0.2% min^{-1}, respectively. Assuming no drift, the sample SEs were a measure of the repeatability. In 30-min tests, the SEs were less than 3% for EOG and 12% for whole-cell recordings.

Table 1 Stability of EOG experiments

T, min	Recordings, #	Traces, #	$V/V_{initial}$ ± SE[a]
3.3	6	60	0.97 ± 0.03
10	2	60	0.99 ± 0.02
13.3	1	40	0.93 ± 0.005
33	1	100	1.11 ± 0.02
57	2	340	0.80 ± 0.08

[a]Mean values of normalized EOG voltage peaks assuming no drift.

Table 2 Stability of whole-cell experiments

T, min	Recordings, #	Traces, #	$I/I_{initial}$ ± SE[a]
10	1	10	0.97 ± 0.02
15	7	105	1.30 ± 0.07
30	6	97	1.24 ± 0.12

[a]Mean values of normalized whole-cell current peaks assuming no drift.

Responses to individual odorants and odorant mixtures

EOG responses to 0.25-s puffs of 16 mM individual odorants, –carvone, +carvone, eugenol, and ethyl butyrate, are shown in Figure 1. Figure 2a,b shows responses to the mixed odorants obtained by EOG and whole-cell recording, respectively. The EOG signal amplitude produced by purified air was much smaller compared with those excited by mixed odorants. The dependence of the relative signal amplitude on odorant mixture concentration is shown in Figure 2c,d. Both dose dependencies saturate at ~10 mM of odorant mixture.

Enhancement by zinc nanoparticles

When olfactory receptor neurons were excited by odorant mixed with suspension of PNCs containing zinc nanoparticles, or with zinc nanoparticles produced from metal rods, the EOG odorant response amplitude was significantly increased. Similar effects were observed whether or not Ca and Mg ions were present (Figure 3). The shape and kinetics of responses in the presence of zinc nanoparticles were similar to those excited by odorant alone. Figure 4a shows an approximate 2.5-fold increase in EOG response amplitude when neurons were excited by an odorant–zinc mixture compared with response evoked by the odorant alone. The incidental increase of EOG peak due to instability cannot be more than 4.5% (Stability and repeatability of olfactory responses); therefore, 2.5-fold increase is significant. The clearing air puffs produced

only small responses. When 2 consecutive odorant puffs generated normal responses, the odorant plus zinc mixture generated the same enhanced response (O + Zn in Figure 4b). When odorant alone is delivered ~5 s after the odorant + zinc mixture, the amplitude of the response was about 40% greater than that evoked by odorant alone (Figure 4b), indicating that not all Zn particles were fully cleared from the receptors. Odorant alone delivered ~10 s after the odorant–zinc mixture generated a normal response, indicating that after 10 s the zinc nanoparticles delivered from the previous puff had cleared the receptors (Figure 4c). Zinc nanoparticles delivered in headspace water vapor (no odorant) evoked responses that were not different from those excited by water vapor or air alone (Figure 5a,b, respectively). The peak EOG amplitude and whole-cell responses to odorant–zinc nanoparticle mixtures (at constant odorant level) increased with the increase of zinc concentration (Figure 6a,b, respectively). The dependence peak amplitude values obtained from traces in Figure 6a,b, as function of zinc concentration, are shown in the panels c and d of Figure 6, respectively.

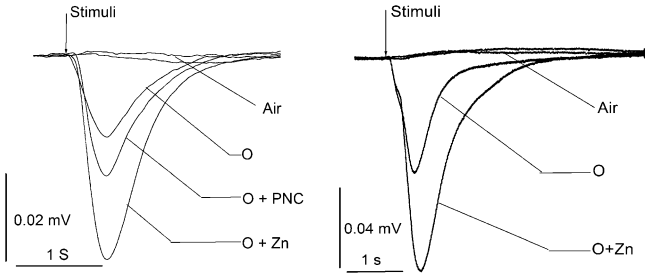

Figure 3 EOG traces from rat OE in Ca- and Mg-free buffer solution (left panel) and in the buffer containing Ca and Mg ions (right panel). Left panel: the responses were induced by air; 16 mM odorants; 16 mM odorants + PNCs (2.2 nM of total Zn); and 16 mM odorant + 5 nM Zn (total Zn). The figure shows representative traces recorded from 1 tissue, 5 contacts, 28 EOG recordings, and 224 traces. Right panel: the responses were induced by air; 16 mM odorants; and 16 mM odorant + 5 nM Zn (total Zn). The figure shows representative traces recorded from 3 rats, 3 tissues, 23 contacts, 55 EOG recordings, and 450 traces.

When olfactory neurons were perfused with a solution containing zinc nanoparticles, the odorant-induced currents changed dramatically (Figure 7a). The initial responses, immediately following perfusion onset, were very similar to those obtained with no zinc nanoparticles. After a few minutes, the EOG peaks became progressively bigger, but the growth slowed after ~70 min of perfusion (Figure 7c). During the first 30 min, the relative EOG responses grew

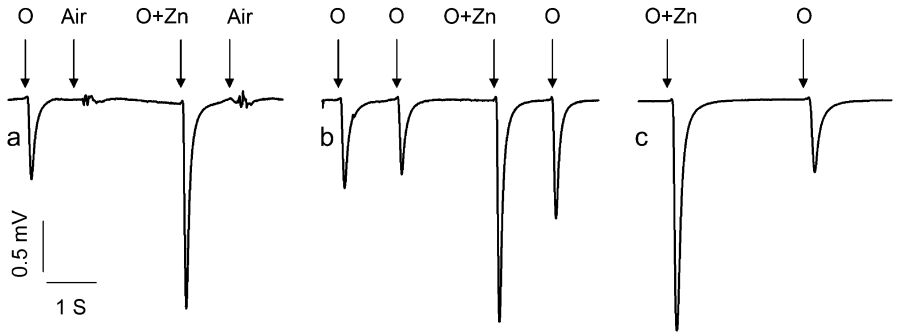

Figure 4 EOG traces from rat OE. The responses were induced by air, 16 mM odorants (O), and mixture of 16 mM odorants and 10 pM zinc metal nanoparticles (O + Zn). Representative traces obtained by a manual control from 1 tissue, 10 contacts, and 39 traces. The stimuli were delivered in the following sequence: **(a)** O, air, O + Zn, air; **(b)** O, O, O + Zn, O; **(c)** O + Zn, O.

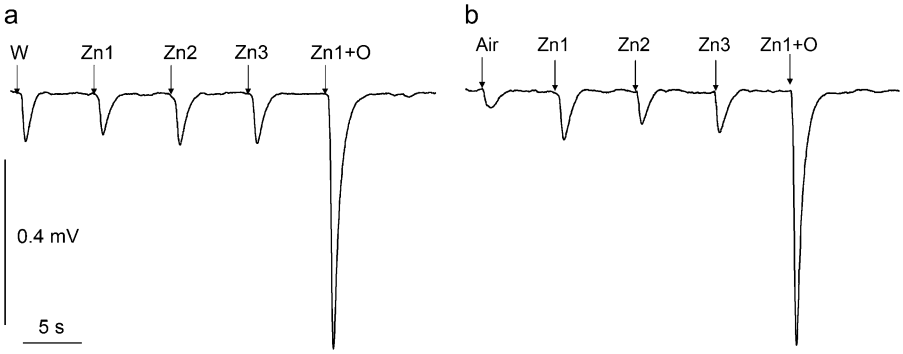

Figure 5 EOG responses elicited by water vapor, air, zinc nanoparticles, and odorant. Representative traces obtained by a manual control from 2 tissues, 6 contacts, and 39 traces. **(a)** The responses were induced by water vapor (W), 6 (Zn1), 60 (Zn2), and 120 (Zn3) pM zinc suspension, and finally with 6 pM zinc plus 16 mM odorant mixture. **(b)** The responses were induced by air (Air), 6 (Zn1), 60 (Zn2), and 120 (Zn3) pM zinc suspension in water, and 6 pM zinc plus 16 mM odorant mixture (Zn1 + O).

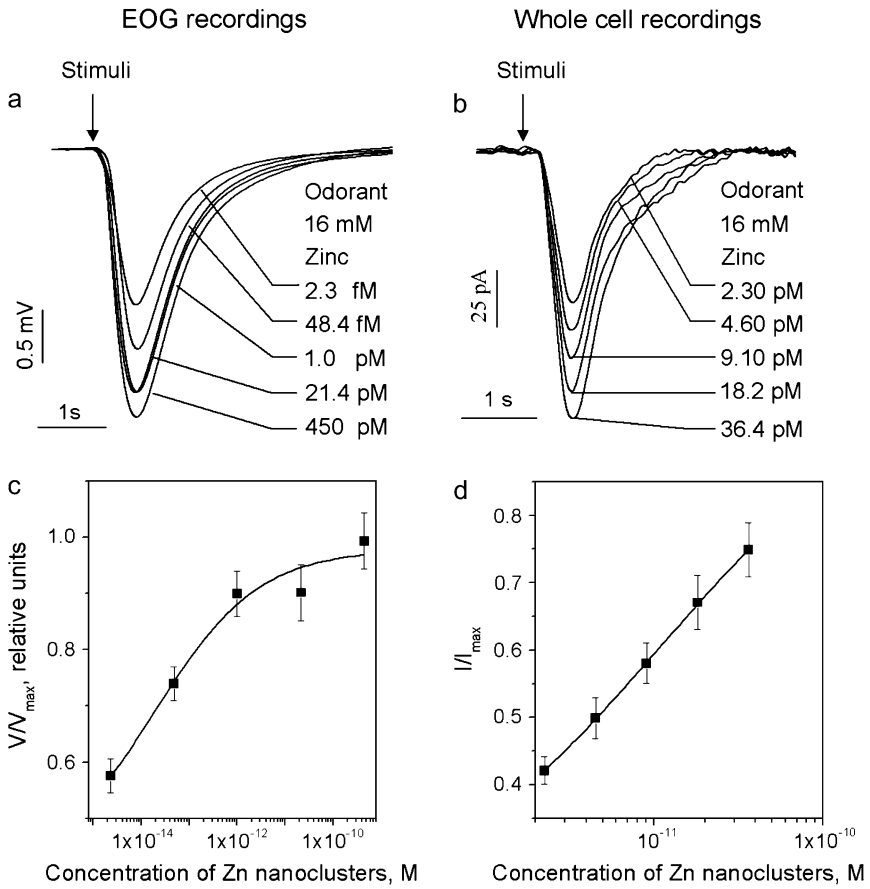

Figure 6 Electrophysiological recordings from rat OE and a single olfactory neuron: odorant + zinc particle responses. The stimulus was a 0.25-s pulse of air or odorant–zinc particle mixture. Odorant concentration was constant for all traces. Odorant vapors were collected above the odorant–zinc suspensions (in water) of zinc concentrations shown in the graphs **(a)**. EOG traces induced by odorant–zinc particle mixture at different concentrations of zinc. Panel (a) shows representative traces obtained in 4 tissues, 10 contacts, and 34 EOG recordings (262 traces). **(b)** Current traces from whole-cell voltage recordings of olfactory neurons with holding potentials of −70 mV. The stimulus was a 0.25-s pulse of odorant–zinc particle mixture. Downward direction indicates inward current. Panel (b) shows representative traces obtained from 23 whole-cell recordings (198 traces). **(c)** Plot of normalized, peak EOG voltage (V/V_{max}) evoked by odorant–zinc particles versus zinc concentration. **(d)** Plot of normalized, peak negative current (I/I_{max}) evoked by odorant–zinc particles versus zinc concentration.

at the rate of 8.1 ± 0.6% min^{-1}, and that was 12 times faster than the average EOG drift rate (see Stability and repeatability of olfactory responses).

When an olfactory neuron was perfused with a patch electrode filled with a solution containing zinc nanoparticles, the odorant-induced currents changed considerably (Figure7b). The initial responses registered at –70 mV immediately after perfusion onset were very similar to those obtained with the patch electrode containing no zinc nanoparticles. But after approximately 4 min, the maximal inward current amplitude grew progressively at the same voltage, puff volume, and puff rate (Figure 7b,d). The whole-cell responses increased at 14.2 ± 0.3% min^{-1}, which rate was 19 times greater than the whole-cell drift rate (see Stability and repeatability of olfactory responses).

Copper, gold, or silver nanoparticles did not produce the effects of Zn (Figure 8). Gold and silver nanoparticles produced a transient enhancement, whereas copper nanoparticles did not change the relative EOG amplitude. When zinc nanoparticles were replaced by Zn^{+2} ions in the same concentration range, the olfactory receptor neuron response to odorant was reduced (Figure 9).

Stability degradation of zinc suspensions occurs through oxidation, aggregation (coarsening), and sedimentation (Goia and Matijevic 1998; Matijevic and Goia 2007). Zinc nanoparticles of different origins in the same concentrations and size ranges produced no detectable differences. However, stability of the suspensions containing zinc nanoparticles of natural origin (PNCs) was higher than those produced artificially from metal zinc (data not shown).

Discussion

Odor enhancement by zinc nanoparticles

We demonstrated that a very small concentration, a few fM to 450 pM, of zinc metal nanoparticles delivered together with odorant can strongly enhance EOG or whole-cell

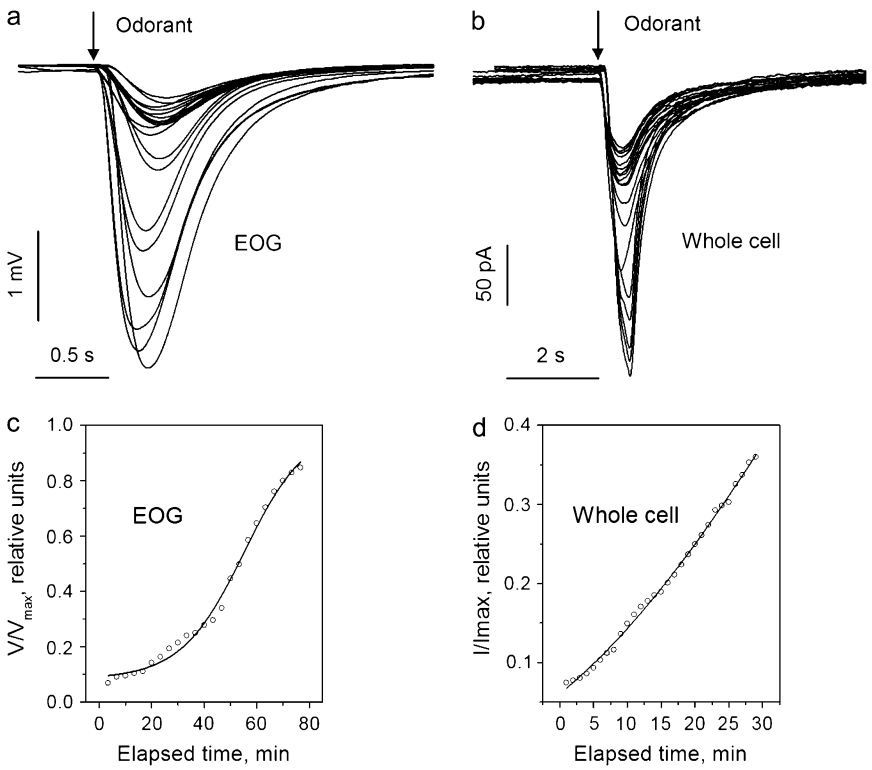

Figure 7 Zinc nanoparticle enhancement of OE response to odorant **(a)**. Superimposed EOG traces stimulated by a 0.25-s, 16 mM odorant mixture puff and a recording made under the same conditions except that the recording pipette contained 5 nM zinc nanoparticles. The first trace was recorded just after contact was made, and the following traces, with the progressively greater amplitude, were recorded at 20-s increments. Panel (a) shows every fifth trace and is representative of traces obtained from 4 tissues, 5 contacts, 61 recordings, and 470 traces. **(b)** Superimposed traces of whole-cell currents stimulated by 0.25-s, 16 mM odorant mixture puffs and traces recorded with the patch-clamp pipette containing 5 nM zinc nanoparticles (holding potentials = −70 mV). The first trace was recorded just after contact was made, and subsequent traces, with the progressively greater amplitude, were recorded in 60-s increments. Panel (b) is representative data from 5 tissues, 48 contacts, 11 recordings, and 460 traces. **(c)** Relative value of peak EOG voltage as function of elapsed time. **(d)** Relative value of peak current of whole-cell odorant response as a function of elapsed time.

patch-clamp responses to odorant. One- to 2-nm metallic nanoparticles contain 40–300 zinc atoms. A small amount of these particles added to an odorant can increase the responses to the odorant by a factor ~2.5 ($N = 39$). Although we cannot find data on the water/vapor (or water/air) partition coefficient for metal nanoparticles, we infer their presence in odorant puffs because the observed effects are dose dependent and reversible. The spontaneous particle clearing from the system provides a specific, sensitive, and effective means of regulation of initial olfactory responses. Zinc nanoparticles enhance olfactory neuron response only if applied in the presence of an odorant but produce no odor effects alone.

When zinc nanoparticles were delivered by extracellular or intracellular perfusion, the EOG and whole-cell patch-clamp responses increased, over time, as much as 7-fold above the initial values. The gradual growth of response amplitude can be explained by the continuing increase of local zinc concentration driven by nanoparticle diffusion. According to the Stokes–Einstein equation, the diffusion coefficient of small nanoparticles can be estimated as $D = kT/6\pi\eta r$, where k is Boltzmann coefficient, T is absolute temperature, η—viscosity, and r—mean hydrodynamic radius of nanoparticles. For the viscosity in a range of 3–11 cP (Keith and Snipes 1974), the diffusion coefficient of 2-nm nanoparticles ($r = 1$ nm) at 300 °K is in a range of 7.4×10^{-7} to 2.0×10^{-7} cm^2 s^{-1}. The nanoparticles can diffuse in the cilia the distance $L = 40$ μm for $L^2/D \cong 20$–80 s. We also estimated that the diffusion time through the pipette's tip that contained no metal nanoparticles is not a rate limiting factor for perfusion of nanoparticles into olfactory neuron. On average, it took 1–3 min to fill a pipette, 1–2 min to position the pipette in the electrode holder, and 1–3 min to make a cell contact. We estimated that the pipette tip was filled to the levels of 250–60 μm. At solution viscosity of 1 cP, the diffusion coefficient is 2.2×10^{-6} cm^2 s^{-1}. Delays of zinc nanoparticle diffusion through the tip are between 5 min and 16 s. Because 5 min is comparable with a mean time spent before making a cell contact, the filling tip containing no zinc solution does not impede the intracellular perfusion of zinc nanoparticles.

The site of action of zinc nanoparticles cannot be determined based only on extracellular and intracellular application efficiency. The metal nanoparticles are electrically neutral and can easily cross the membrane to the location of activity. In contrast with ions, nanoparticles do not need

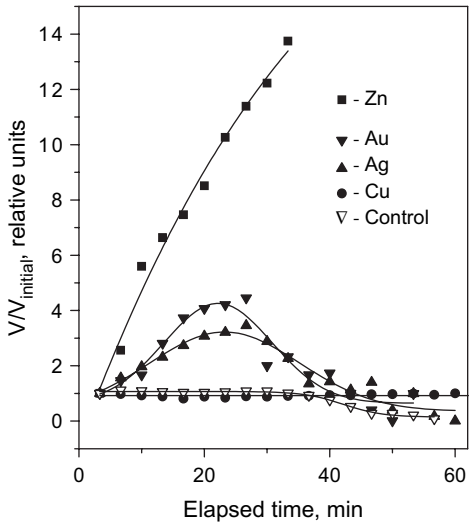

Figure 8 Metal nanoparticle effects on the odorant-induced OE response. Relative EOG amplitude stimulated by 0.25-s puff of 16 mM odorant mixture and recorded from OE. The recording pipette contained 5 nM zinc, gold, silver, or copper metal nanoparticles. Control contained no metal particles. The first trace for each metal was recorded just after contact was made, and the subsequent traces were made at 200-s intervals. Data were obtained from zinc: 3 tissues, 4 contacts, 60 recordings, and 450 traces; gold: 1 tissue, 2 contacts, 28 recordings, and 221 traces; silver: 2 tissues, 4 contacts, 58 recordings, and 460 traces; copper: 1 tissue, 2 contacts, 23 recordings, and 172 traces; control: 2 tissues, 37 recordings, and 340 traces.

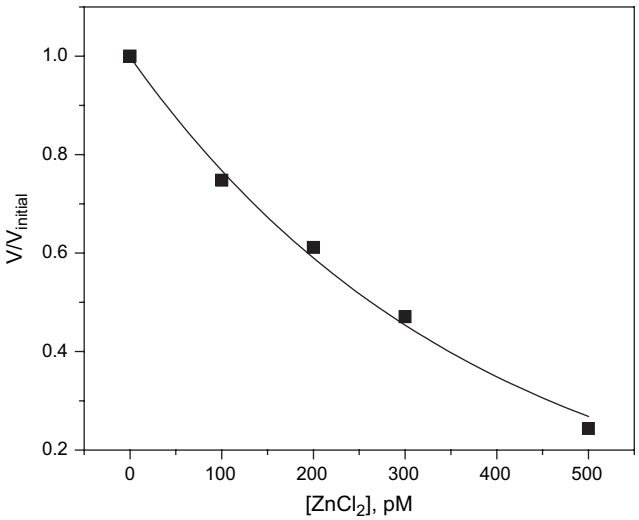

Figure 9 Effects of Zn^{+2} ions on the odorant response. Relative value of peak EOG voltage as function of $ZnCl_2$ concentration. The initial EOG peak voltage, $V_{initial}$ = −0.15 mV, was obtained from 0.16 mM odorant mixture alone, whereas the other points were obtained from mixed solutions of odorants and $ZnCl_2$. Odorant concentration was constant. Points are the experimental results, and the curve is the exponential fit (χ^2 = 0.0006, R^2 = 0.995, τ = 380 pM). Representative data from 12 tissues, 23 contacts, 95 recordings, and 757 traces.

channels to cross the membrane, and they are not controlled by membrane potentials. Therefore, nanoparticles can cross the membrane in a very short time, and we can estimate the diffusion coefficient using the Stokes–Einstein equation. If the membrane viscosity is equal to 1.0 P (Miyamoto et al. 1990), the diffusion coefficient of 2-nm nanoparticles at 300 °K is 1.1×10^{-12} cm^2 s^{-1}. These nanoparticles can cross a membrane (10–30 nm) in 90–800 μs (less than 1 ms), and we observed, by transmission electron microscopy, nanoparticles on the cytoplasmic side of the membrane following application to tissue preparations (Samoylov et al. 2005).

There is a significant difference between zinc ions and zinc nanoparticles. A zinc ion is a single atom that lost 2 electrons to make it positively charged. The metal zinc nanoparticle is comprised of a relatively large number of neutral atoms. For example, 1-nm zinc nanoparticles contain ~40 atoms, but 2-nm particle has ~300 atoms. The physical, chemical, and catalytic properties of metal nanoparticles are different from those of ions and bulk metals (Thomas 1988; Aiken and Finke 1999).

When zinc nanoparticles were delivered together with an odorant vapor pulse, the effect of nanoparticles seemed to be very rapid and did not produce delays in inward currents excited by the odorant–zinc mixture compared with inward currents evoked by odorant alone (Figures 3 and 6). This fact indicates that zinc nanoparticles arrive at the place of action almost simultaneously with the odorant molecules' arrival at their receptors. Because the latency between stimulus arrival and onset of current is no longer than 160 ms (Grosmaitre et al. 2006), zinc nanoparticles are not diffusing far before they reach their site of action. There is a well-defined sequence of biochemical events between odorant arrival at olfactory cilia and ion current generation. Transduction begins with odorant receptor protein binding (Buck and Axel 1991). This interaction results in G_{olf} disengagement from the intracellular receptor protein domain (Jones and Reed 1989). Subsequently, G_{olf} dissociates into 3 subunits, α, β, and γ, with the activation of a type III AC (Bakalyar and Reed 1990) by the $G_{olf\text{-}\alpha}$ subunit (Sinnarajah et al. 1998). AC then elevates the concentration of cAMP that gates cyclic nucleotide–gated channels (Nakamura and Gold 1987). The inward flow of Ca^{2+} ions in turn gates Ca^{2+}-activated Cl^- channels (Kleene 1993, 2002; Kurahashi and Yau 1993). The components of the signal transduction cascade are probably located in close proximity to each other. We infer such a spatial array because small fragments of disrupted OE cilia that are reconstituted into artificial bilayers exhibit most of the biochemical events of the intact system (Vodyanoy and Murphy 1983; Vodyanoy V and Vodyanoy I 1987a, 1987b; Vodyanoy 1991; Sinnarajah et al. 1998).

Hypothetically, zinc nanoparticles that arrive with odorant at the cilia can modulate any of the signal transduction cascade events. We found no reports in the literature related to zinc nanoparticles and olfaction. The enhancement of

odorant responses by zinc nanoparticles was observed even at saturated odorant concentrations (Figure 6c,d). If we assume that at saturated odorant concentration, all odorant receptor sites are occupied and zinc nanoparticles that arrive together with odorant molecules cannot increase the number of odorant-binding sites. How then can zinc nanoparticles facilitate the transduction? According to the Luca Turin's model (Turin 1996), endogenous zinc ions provide a bridge connecting receptor and G_{olf}-proteins. When a proper odorant binds a coupled receptor–G_{olf} complex, G_{olf} is decoupled and initiates the rest of the transduction cascade. We hypothesize that zinc nanoparticles instead of zinc ions facilitate coupling of odorant receptors and G_{olf}. The odorant response of OE neurons at saturated odorant concentration depends on the number of receptor–G_{olf} couplings that is in turn a function of the concentration of endogenous zinc nanoparticles. We speculate that by adding zinc nanoparticles, we increase the number of receptor–G_{olf} couplings and therefore enhance the olfactory response.

It has been reported that the odorant dwell time on odorant receptor is very short (on the order of 1 ms) (Bhandawat et al. 2005). The receptor–G_{olf} couplings are too short lived to explain both activation of G_{olf} and phosphorylation by G-protein–coupled receptor kinases, which could uncouple receptor–G-protein interactions (Boekhoff et al. 1992). We speculate that zinc nanoparticles may play an important role in controlling the receptor–G_{olf} coupling.

The fact of odorant response enhancement by a small zinc particle positioned between the receptor and G_{olf} is consistent with Luca Turin's (Turin 1996) suggestion that zinc ion–binding sites are present both on the odorant receptor protein and the G-protein and that zinc ions assist the signal transfer from receptor to G-protein. These zinc metal particles can work also as electron donors as predicted by the general theoretical model of Brookes et al. (2007).

Criteria for physiological significance of zinc nanoparticles

If zinc nanoparticles act through olfactory receptors to enhance an odorant-mediated cascade in olfactory cilia, then we need to demonstrate certain criteria to establish their physiological role. These criteria are similar to those suggested for justifying claims that a given effector produces its effect as a result of the stimulation of AC (Robinson 1971; Menevse et al. 1977; Vodyanoy V and Vodyanoy I 1987b; Sinnarajah et al. 1998). The main criteria are as follows: (i) olfactory sensory neurons should contain zinc nanoparticles, (ii) the activity of olfactory sensory neurons is modulated by zinc nanoparticles, and (iii) modulation of olfactory sensory neurons does not occur if zinc nanoparticles are removed or replaced.

Criterion (i) is supported to some extent by the fact that free and bound zinc is found in relatively large concentrations in the OE, the olfactory bulb, as well as other parts of the brain (Horning and Trombley 2001; Takeda 2001; Persson et al. 2003; Frederickson et al. 2006). Criterion (ii) is fully supported by the experimental results presented here. We demonstrated significant modulation of the olfactory sensory neurons' activity, manifested by an odorant response enhancement when zinc nanoparticles are present. Criterion (iii) is met because the enhancement of odorant responses does not occur if zinc nanoparticles are replaced by zinc ions. We could not find any reports in literature on the presence of zinc nanoparticles in olfactory cilia and effects of zinc nanoparticles on the activity of olfactory sensory neurons. Therefore, the physiological significance of zinc nanoparticles may be established only if direct evidence of zinc nanoparticles' presence in olfactory cilia is demonstrated and our electrophysiological results are replicated by other laboratories.

The important role of zinc nanoparticles in olfactory transduction is a further illustration of the significant role of zinc in neurobiology (Frederickson et al. 2005). In most cases, the distribution of zinc in the brain was studied by methods that cannot discriminate between zinc ions and zinc metal particles (Takeda et al. 1997; Takeda 2001). Zinc transporters in brain are known (Takeda 2001), but it is not known if the same system of zinc homeostasis supports zinc nanoparticles. Small colloidal metal particles were studied by 19th century colloidal science (Kruyt 1952; Thomas 1988), and then with more advanced methods of chemistry and physics in the 20th century, the small metal particles, called metal nanoclusters, were better understood and used in the rapidly developing field of nanotechnology (Jena et al. 1996; Aiken and Finke 1999). Very recently, metal nanoparticles, now called superatoms, have been intensively studied (Hakkinen 2008; Walter et al. 2008; Castleman and Khanna 2009). Superatoms have special electronic structures and thereby possess unusual chemical and physical properties, which may include resistance to aggregation and oxidation. We found a large number of stable metal nanoparticles in human and animal blood (Samoylov et al. 2005), but the observations reported herein are the first to suggest any physiological significance.

Funding

Fetzer Institute Inc., (grant #2231); Department of Homeland Security, Science and Technology Directorate (grant #01-G-022).

Acknowledgements

Authors are grateful to Ms Nancy Morrison for helping with physiological characterization of PNC and zinc nanoparticles.

References

Aiken JD, Finke RG. 1999. A review of modern transition-metal nanoclusters: their synthesis, characterization, and applications in catalysis. J Mol Catal a Chem. 145:1–44.

Anholt RRH, Mumby SM, Stoffers DA, Girard PR, Kuo JF, Snyder SH. 1987. Transduction proteins of olfactory receptor-cells—identification of guanine-nucleotide binding-proteins and protein-kinase-C. Biochemistry. 26:788–795.

Bakalyar HA, Reed RR. 1990. Identification of a specialized adenylyl cyclase that may mediate odorant detection. Science. 250:1403–1406.

Bhandawat V, Reisert J, Yau K-W. 2005. Elementary response of olfactory receptor neurons to odorants. Science. 308:1931–1934.

Boekhoff I, Schleicher S, Strotmann J, Breer H. 1992. Odor-induced phosphorylation of olfactory cilia proteins. Proc Natl Acad Sci USA. 89:11983–11987.

Breer H. 1994. Signal recognition and chemoelectrical transduction in olfaction. Biosens Bioelectron. 9:625–632.

Brookes JC, Hartoutsiou F, Horsfield AP, Stoneham AM. 2007. Could humans recognize odor by phonon assisted tunneling? Phys Rev Lett. 98:038101-1–038101-4.

Buck L, Axel R. 1991. A novel multigene family may encode odorant receptors—a molecular-basis for odor recognition. Cell. 65:175–187.

Castleman AW, Khanna SN. 2009. Clusters, superatoms, and building blocks of new materials. J Phys Chem C. 113:2664–2675.

Fadool DA, Ache BW. 1992. Plasma-membrane inositol 1,4,5-trisphosphate-activated channels mediate signal transduction in lobster olfactory receptor neurons. Neuron. 9:907–918.

Firestein S, Picco C, Menini A. 1993. The relation between stimulus and response in olfactory receptor-cells of the tiger salamander. J Physiol. 468:1–10.

Frederickson CJ, Giblin LJ, Krezel A, McAdoo DJ, Muelle RN, Zeng Y, Balaji RV, Masalha R, Thompson RB, Fierke CA, et al. 2006. Concentrations of extracellular free zinc (pZn)(e) in the central nervous system during simple anesthetization, ischemia and reperfusion. Exp Neurol. 198:285–293.

Frederickson CJ, Koh JY, Bush AI. 2005. The neurobiology of zinc in health and disease. Nat Rev Neurosci. 6:449–462.

Goia DV, Matijevic E. 1998. Preparation of monodispersed metal particles. New J Chem. 22:1203–1215.

Grosmaitre X, Vassalli A, Mombaerts P, Shepherd GM, Ma MH. 2006. Odorant responses of olfactory sensory neurons expressing the odorant receptor MOR23: a patch clamp analysis in gene-targeted mice. Proc Natl Acad Sci USA. 103:1970–1975.

Hakkinen H. 2008. Atomic and electronic structure of gold clusters: understanding flakes, cages and superatoms from simple concepts. Chem Soc Rev. 37:1847–1859.

Horning MS, Trombley PQ. 2001. Zinc and copper influence excitability of rat olfactory bulb neurons by multiple mechanisms. J Neurophysiol. 86: 1652–1660.

Jena P, Khanna SN, Rao BK. 1996. Stability and electronic structure of cluster assembled materials. In: Sattler K, editor. Cluster Assembled Materials. Vol. 232. Zurich: Trans Tech Publications. p. 1–25.

Jones DT, Reed RR. 1989. Golf—an olfactory neuron specific G-protein involved in odorant signal transduction. Science. 244:790–795.

Keith AD, Snipes W. 1974. Viscosity of cellular protoplasm. Science. 183: 666–668.

Kleene SJ. 1993. Origin of the chloride current in olfactory transduction. Neuron. 11:123–132.

Kleene SJ. 2002. The calcium-activated chloride conductance in olfactory receptor neurons. Curr Top Membr. 53:119–134.

Kruyt HR. 1952. Colloid science. New York: Elsevier.

Kurahashi T, Yau KW. 1993. Co-existence of cationic and chloride components in odorant-induced current of vertebrate olfactory receptor cells. Nature. 363:71–74.

Ma MH, Chen WR, Shepherd GM. 1999. Electrophysiological characterization of rat and mouse olfactory receptor neurons from an intact epithelial preparation. J Neurosci Methods. 92:31–40.

Matijevic E, Goia D. 2007. Formation mechanisms of uniform colloid particles. Croat Chem Acta. 80:485–491.

Menevse A, Dodd G, Poynder TM. 1977. Evidence for specific involvement of cyclic-amp in olfactory transduction mechanism. Biochem Biophys Res Commun. 77:671–677.

Miyamoto A, Araiso T, Koyama T, Ohshika H. 1990. Membrane viscosity correlates with adrenergic signal transduction of the aged rat cerebral cortex. J Neurochem. 55:70–75.

Nakamura T, Gold GH. 1987. A cyclic nucleotide-gated conductance in olfactory receptor cilia. Nature. 325:442–444.

Pace U, Hanski E, Salomon Y, Lancet D. 1985. Odorant-sensitive adenylate-cyclase may mediate olfactory reception. Nature. 316: 255–258.

Persson E, Henriksson J, Tallkvist J, Rouleau C, Tjälve H. 2003. Transport and subcellular distribution of intranasally administered zinc in the olfactory system of rats and pikes. Toxicology. 191:97–108.

Robinson GA. 1971. Cyclic AMP. New York: Academic Press.

Samoylov AM, Samoylova TI, Pustovyy OM, Samoylov AA, Toivio-Kinnucan MA, Morrison NE, Globa LP, Gale WF, Vodyanoy V. 2005. Novel metal clusters isolated from blood are lethal to cancer cells. Cells Tissues Organs. 179:115–124.

Sinnarajah S, Dessauer CW, Srikumar D, Chen J, Yuen J, Yllma S, Dennis JC, Morrison EE, Vodyanoy V, Kehrl JH. 2001. RGS2 regulates signal transduction in olfactory neurons by attenuating activation of adenylyl cyclase III. Nature. 409:1051–1055.

Sinnarajah S, Ezeh PI, Pathirana S, Moss AG, Morrison EE, Vodyanoy V. 1998. Inhibition and enhancement of odorant-induced cAMP accumulation in rat olfactory cilia by antibodies directed against Gas/olf- and Gai-protein subunits. FEBS Lett. 426:377–380.

Sklar PB, Anholt RRH, Snyder SH. 1986. The odorant-sensitive adenylate-cyclase of olfactory receptor-cells—differential stimulation by distinct classes of odorants. J Biol Chem. 261:5538–5543.

Takeda A. 2001. Zinc homeostasis and functions of zinc in the brain. Biometals. 14:343–351.

Takeda A, Ohnuma M, Sawashita J, Okada S. 1997. Zinc transport in the rat olfactory system. Neurosci Lett. 225:69–71.

Thomas JM. 1988. Colloidal metals—past, present and future. Pure Appl Chem. 60:1517–1528.

Turin L. 1996. A spectroscopic mechanism for primary olfactory reception. Chem Senses. 21:773–791.

Viswaprakash N, Dennis JC, Samoylov AM, Josephson EM, Morrison EE, Vodyanoy V. 2006. Enhancement of odorant-induced responses in olfactory receptor neurons by zinc nanoclusters. Society for Neuroscience Annual Meeting. Atlanta (GA): Society for Neuroscience. Available from: URL http://www.abstractsonline.com/viewer/SearchResults.asp. Abstract number 355.16/Z30.

Vodyanoy V. 1991. Cyclic AMP-sensitive ion channels in olfactory receptor cells. Chem Senses. 16:175–180.

Vodyanoy V, Murphy RB. 1983. Single-channel fluctuations in bimolecular lipid-membranes induced by rat olfactory epithelial homogenates. Science. 220:717–719.

Vodyanoy V, Vodyanoy I. 1987a. ATP and GTP are essential for olfactory response. Neurosci Lett. 73:253–258.

Vodyanoy V, Vodyanoy I. 1987b. The role of ATP and GTP in the mediation of the modulatory effects of odorant on olfactory receptor-sites functionally reconstituted into planar lipid bilayers. Ann N Y Acad Sci. 510:683–686.

Walter M, Akola J, Lopez-Acevedo O, Jadzinsky PD, Calero G, Ackerson CJ, Whetten RL, Gonbeck H, Hakkinen H. 2008. A unified view of ligand-protected gold clusters as superatom complexes. Proc Natl Acad Sci USA. 105:9157–9162.

Accepted May 14, 2009